Anthraquinone catalysis in the glucose-driven reduction of indigo to *leuco*-indigo

Anne Vuorema,[a] Philip John,[b] Marjo Keskitalo,[a] Mary F. Mahon,[c] M. Anbu Kulandainathan[d] and Frank Marken*[c]

Received 14th August 2008, Accepted 1st December 2008
First published as an Advance Article on the web 14th January 2009
DOI: 10.1039/b814149e

Anthraquinone immobilised onto the surface of indigo microcrystals enhances the reductive dissolution of indigo to *leuco*-indigo. Indigo reduction is driven by glucose in aqueous NaOH and a vibrating gold disc electrode is employed to monitor the increasing *leuco*-indigo concentration with time. Anthraquinone introduces a strong catalytic effect which is explained by invoking a molecular "wedge effect" during co-intercalation of Na^+ and anthraquinone into the layered indigo crystal structure. The glucose-driven indigo reduction, which is ineffective in 0.1 M NaOH at 65 °C, becomes facile and goes to completion in the presence of anthraquinone catalyst. Electron microscopy of indigo crystals before and after reductive dissolution confirms a delamination mechanism initiated at the edges of the plate-like indigo crystals. Catalysis occurs when the anthraquinone–indigo mixture reaches a molar ratio of 1 : 400 (at 65 °C; corresponding to 3 μM anthraquinone) with excess of anthraquinone having virtually no effect. A strong temperature effect (with a composite $E_A \approx 120$ kJ mol^{-1}) is observed for the reductive dissolution in the presence of anthraquinone. The molar ratio and temperature effects are both consistent with the heterogeneous nature of the anthraquinone catalysis in the aqueous reaction mixture.

1. Introduction

For centuries indigo has been a popular dye,[1] the current annual world consumption of indigo and other vat dyes being about 33 million kg.[2] Indigo as a vat dye requires that the water-insoluble oxidised form is reduced to its water-soluble *leuco*-form prior to the dyeing process. Traditionally, a fermenting woad bath was used to reduce indigo.[3] Anthraquinone-containing madder extracts were invariably added to this bath, and it has been shown with pure cultures of the indigo-reducing bacterium *Clostridium isatidis*, that soluble anthraquinones stimulate bacterial indigo reduction.[4,5] With the replacement of natural indigo by the synthetic product at the end of the 19th century, the bacterial fermentation bath was replaced by sodium dithionite, which for a long time was the sole industrial reducing agent. But recently, a plethora of less environmentally harmful reducing agents and processes have been developed[6–10] among which direct or indirect (mediated) electrochemical methods are perhaps the most significant. Mediator-based electrochemical reactions with the Fe(III) triethanolamine (TEA) complex,[11] Fe(III) Hedta,[12] with Fe^{3+}-D-gluconate or Ca^{2+}–Fe^{3+}-D-gluconate complexes,[13] and with anthraquinone derivatives[14] have been studied. Direct reduction processes of indigo in fixed and fluidised beds,[15] or at nickel contacts[16] represent alternative mediator-free approaches.

Glucose has been investigated for sulfur dye reduction processes[17] and it is considered to be a possible benign alternative reducing agent for indigo.[18] Glucose is degraded in alkaline solutions in a complex sequence of reaction steps[19–21] and the reducing effect of glucose is associated with a not-fully-characterised electron-rich intermediate.[22] We have recently demonstrated that the glucose-driven reductive dissolution of indigo can also be catalysed in the presence of anthraquinone derivatives such as the water-soluble 1,8-dihydroxyanthraquinone.[18] The use of this catalyst allows for lower levels of added alkali and for lower operating temperatures during reductive dissolution. Anthraquinones can be electrochemically reduced in aqueous alkaline solution at a potential similar to that for the reduction of indigo, forming the two-electron two-proton anthraquinol product, which then transfers electrons to the suspended indigo. Usually, a soluble anthraquinone derivative is used as catalyst. However, the parent anthraquinone compound is not water-soluble and the alkali metal salts of the parent anthraquinol exhibit only limited water-solubility.[23] Two major benefits of the parent anthraquinone compared to other more soluble anthraquinone derivatives are slightly lower toxicity and lower cost. It is shown here that the parent anthraquinone is a highly effective catalyst for indigo reduction and that the low solubility of anthraquinone during the indigo reduction process actually is a beneficial feature.

In this study, the catalytic effect of the water-insoluble anthraquinone on the reductive dissolution of indigo is studied quantitatively. Electrochemical experiments are reported that monitor the formation of *leuco*-indigo. The anthraquinone

[a] *MTT Agrifood Research Finland, Plant Production Research, Crop Science and Technology, FIN-31600 Jokioinen, Finland*
[b] *School of Biological Sciences, The University of Reading, PO Box 221, Reading, UK RG6 6AS*
[c] *Department of Chemistry, University of Bath, Bath, UK BA2 7AY. E-mail: f.marken@bath.ac.uk*
[d] *Electro-organic Division, Central Electrochemical Research Institute, Karaikudi, 630 006, India*

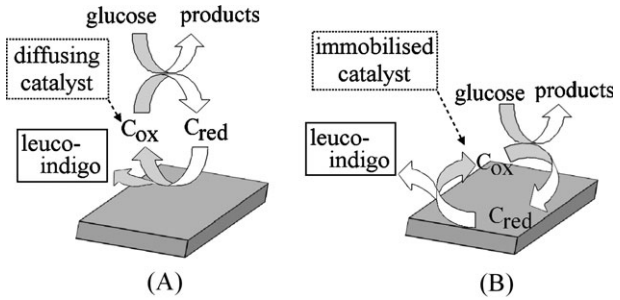

Fig. 1 Schematic representation for (A) solution phase catalysis and (B) surface catalysis mechanisms for the glucose-driven reduction of indigo to *leuco*-indigo.

catalyst is immobilised onto the indigo micro-crystal surface prior to the glucose-driven indigo reduction process. The schematic drawings in Fig. 1 compare the case of (A) a solution soluble catalyst affecting the indigo reduction and (B) a surface immobilised catalyst. The latter case allows catalyst to be effective only at the point where the reaction occurs.

Kinetic data for the indigo reduction are obtained with a vibrating electrode system which allows the *leuco*-indigo content to be monitored. The effect of the reductive indigo dissolution on the crystal morphology is investigated by monitoring indigo crystals (grown by sublimation) with scanning electron microscopy.

2. Experimental

2.1 Reagents

Chemical reagents including indigo (Fluka), NaOH (Aldrich), anthraquinone (Sigma), acetone (Sigma), and D-(+)-glucose (Sigma), were obtained commercially and used without further purification. Demineralised water was taken from an Elga purification system with at least 18 MΩ cm resistivity. Argon (BOC) gas was employed for solution de-aeration.

2.2 Instrumentation

For voltammetric studies a micro-Autolab II potentiostat system (EcoChemie, Netherlands) was employed with a Pt wire counter electrode and a saturated Calomel (SCE) reference electrode (Radiometer, Copenhagen). Solid-state electrochemical experiments were carried out with a 4.9 mm diameter basal plane pyrolytic graphite electrode (Le Carbon, UK). A 500 μm diameter vibrating gold disc electrode acted as a working electrode for the quantitative determination of *leuco*-indigo. The electrode was embedded in a home-build PEEK probe connected to a sonic probe (Braun, Oral-B Sonic Complete, 250 Hz) to produce a sonic vibration with approximately ±*ca.* 200 μm amplitude[24] (see Fig. 2).

Experiments were conducted in a thermostated electrochemical cell (with a Haake B3 circulator) under constant de-aeration with high purity argon.

2.3 Procedure for solid-state electrochemical measurements

Aqueous 0.1 M NaOH was thermostated to 20, 55, 65 or 75 °C and microcrystals of indigo or anthraquinone were immobilised at the basal plane pyrolytic graphite electrode by rubbing on a filter paper.[25,26] The electrode was then immersed into solution and cyclic voltammograms recorded for a range of different scan rates. Each measurement consisted of four consecutive potential cycles to explore the time-dependent reductive dissolution of *leuco*- product away from the electrode surface.

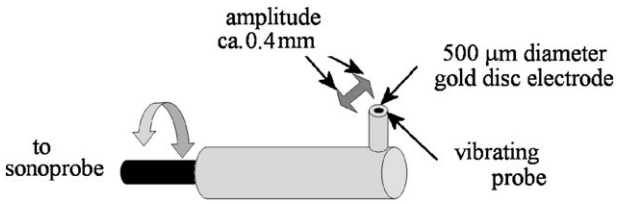

Fig. 2 Schematic drawing of the 250 Hz vibrating electrode system used to measure *leuco*-indigo content during reduction in aqueous media with glucose as the reducing reagent.

2.4 Procedure for the voltammetric determination of *leuco*-indigo

Anthraquinone catalyst was immobilised onto indigo particles by adding an acetone solution (concentration 0.3 mM) to solid indigo powder. The suspension was homogenised with 24 kHz ultrasound (Hielscher UP200G) and the acetone solvent was evaporated to leave anthraquinone coated onto the indigo powder.

An aqueous NaOH solution (100 cm^3) was thermostated to 55, 65 or 75 °C and 30 mg indigo added (corresponding to 1.1 mM solution) after pre-dispersion in a small volume of solution by treatment with 24 kHz ultrasound. Next, 400 mg glucose (corresponding to 22 mM solution in 100 cm^3 of NaOH) was added under an atmosphere of argon and voltammograms (limiting currents for the oxidation of *leuco*-indigo) at the vibrating gold disc electrode[24] were recorded at regular time intervals. Polishing the gold electrode surface before each measurement was required.

2.5 Procedure for indigo sublimation and SEM

Indigo crystals were formed following sublimation in a short path vacuum sublimation system (made from glass) with internal water-cooled deposition finger. The system was heated in silicone oil to a temperature of ~240 °C. Sublimation under oil pump vacuum (*ca.* 10^{-3} Torr) was continued for 3 days (nights excluded). Macroscopic but very thin plate-like indigo crystals were obtained (see Fig. 3). Indigo crystals were collected and attached to the double-sided conducting carbon sticky pads for SEM, which were mounted on glass slides. The glass slide with indigo crystal samples were immersed in the reduction solution (33 mM glucose in 0.2 M NaOH at 65 °C). Samples of indigo, exposed to reducing conditions for different lengths of time, were rinsed in water, dried, and used directly for electron microscopy (after gold sputter coating).

In order to apply anthraquinone catalyst, a 0.3 mM anthraquinone solution in acetone (*ca.* 0.1 cm^3) was added to indigo crystal samples (*ca.* 10 mg) and allowed to evaporate. The catalyst-impregnated indigo crystals were then mounted, reacted, and imaged as before.

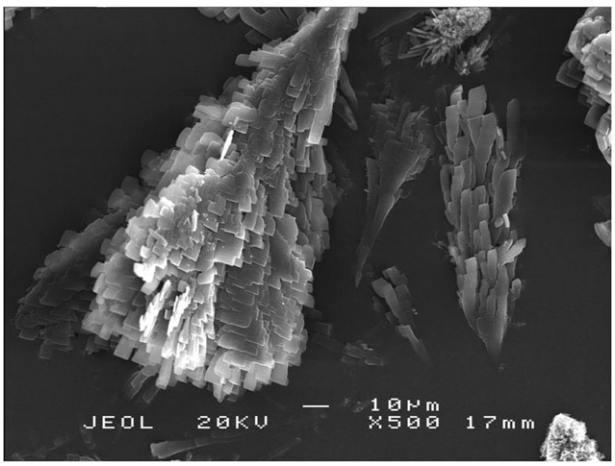

Fig. 3 Typical scanning electron microscopy (SEM) image of the plate-like indigo micro-crystals grown by sublimation and immobilised onto double sided carbon tape.

3. Results and discussion

3.1 Solid-state voltammetry study of the temperature-dependent reduction of indigo and anthraquinone

Indigo is a highly water-insoluble material due to strong hydrogen-bonding interactions in the layered solid state structure.[27] The industrial reduction of indigo (and other vat-dyes) is performed in alkaline aqueous environments in order to dissolve the 2-electron reduction product *leuco*-indigo (pK_{a1} = 8.0, pK_{a2} = 12.7[28]) for the vat-dyeing process.[29] The solid state electrochemistry of indigo micro-particles immobilised at graphite electrodes has been previously reported in the literature for aqueous media[30] and for non-aqueous media.[31] The aqueous process has been shown to be highly pH-dependent. At a pH < 13 a reversible 2-electron 2-proton process occurs without significant dissolution of indigo. Only at significantly more negative potentials does a further Na^+-cation-dependent intercalation process occur, which ultimately causes the break-up of the indigo solid[30] during reductive dissolution. At pH 13 these two processes, based on H^+ and Na^+, merge into a single reductive dissolution response, but even then the dissolution of indigo remains rate-limited by the relatively slow dissolution process.[30]

Fig. 4A shows typical cyclic voltammograms obtained for solid indigo particles immobilised at a basal plane pyrolytic graphite electrode surface immersed in aqueous 0.1 M NaOH. The reversible reduction response at −0.75 V *vs.* SCE is consistent with the 2-electron reduction of indigo to *leuco*-indigo. The shape of the voltammetric signal is complex with a peak superimposed on a slower constant process. A minor oxidation response at −0.1 V *vs.* SCE has been attributed to the 2-electron oxidation of indigo.[30]

The reduction of solid indigo immobilised at a basal plane pyrolytic graphite electrode is strongly temperature-dependent. Fig. 4A shows voltammograms obtained at 20 °C, 55 °C, 65 °C, and 75 °C. The cathodic current response increases with temperature and this suggests that the rate of the dissolution process is increased. An Arrhenius-type plot (see inset, Fig. 4B) reveals an approximate activation energy of 14 kJ mol^{-1}. The

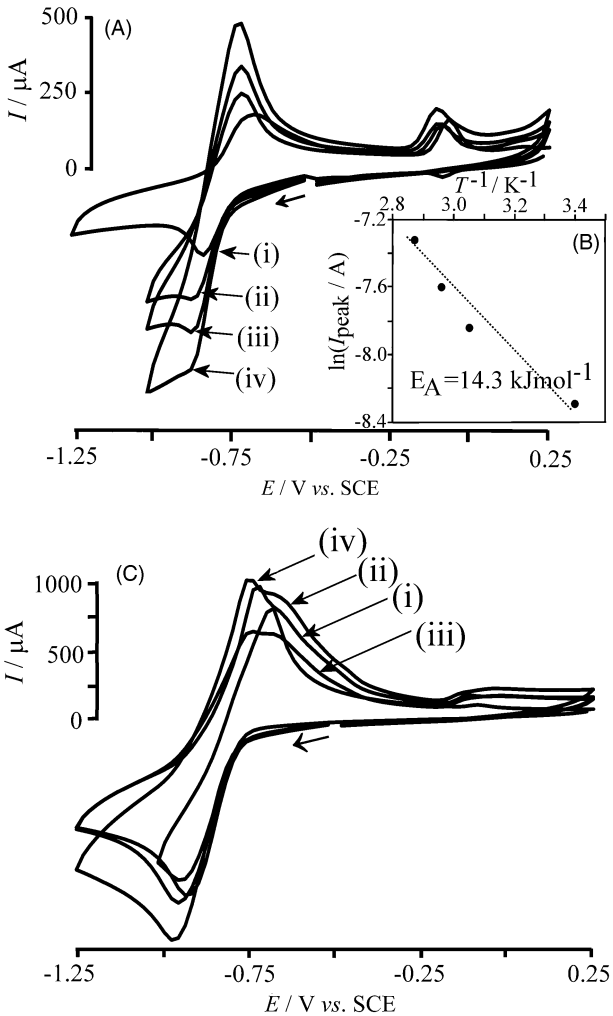

Fig. 4 Solid-state voltammetry data (scan rate 0.2 V s^{-1}) (A) for the reduction of indigo microcrystals and (C) for the reduction of anthraquinone microcrystals immobilised at a basal plane pyrolytic graphite electrode and immersed in aqueous 0.1 M NaOH. Data were obtained at temperatures (i) 20 °C, (ii) 55 °C, (iii) 65 °C, and (iv) 75 °C. (B) Arrhenius plot of the indigo reduction peak current *versus* T^{-1}.

process may be limited by the rate of sodium cations diffusing into the reaction zone, *e.g.* the edges of the indigo lattice (*vide infra*). Cyclic voltammograms obtained over a range of scan rates (0.05 to 2.0 V s^{-1}, not shown) show an increase in the peak current (but not in the underlying step) at higher scan rate.

In contrast to the temperature-dependent characteristics observed for the reduction of solid immobilised indigo, microparticles of anthraquinone immobilised at a basal plane pyrolytic graphite electrode show a reversible reduction response at *ca.* −0.85 V *vs.* SCE without a significant temperature effect. The process is consistent with the 2-electron reduction of anthraquinone.[32] The anthraquinol product appears to be sufficiently water insoluble to remain at the electrode surface. Cyclic voltammetry experiments conducted over a range of scan rates (0.05 to 2.0 V s^{-1}, not shown) reveal increased irreversibility at 65 °C and 75 °C (where loss due to diffusion away from the electrode becomes noticeable) at scan rates of less than 0.1 V s^{-1}. The relatively insignificant

temperature effect on the voltammetric response suggests a facile solid-state conversion which is approaching completion.

The reversible reduction potential for solid anthraquinone appears to be *ca.* 100 mV negative of that for solid indigo (in aqueous 0.1 M NaOH) and therefore anthraquinone should be an effective redox mediator and catalyst for indigo reduction.

3.2 Monitoring the glucose-driven reduction of indigo to *leuco*-indigo at vibrating gold electrodes

The progress of the reduction of solid indigo can be monitored conveniently by measuring the solution concentration of *leuco*-indigo. A reliable methodology based on a vibrating gold electrode has been developed recently.[24] In this method, fast mass transport at the surface of a vibrating (250 Hz) gold disc electrode (500 μm diameter) is exploited for the steady-state mass-transport-limited determination of the *leuco*-indigo concentration in solution.

Fig. 5A shows an overlay of cyclic voltammograms (as a function of time) recorded during the reduction of indigo by glucose. Upon scanning the potential of the vibrating electrode from −1.0 V *vs.* SCE positive, a sigmoidal oxidation response occurs at −0.65 V *vs.* SCE consistent with the oxidation of *leuco*-indigo to indigo. A plateau current is observed and the limiting current is determined at −0.6 V *vs.* SCE (see P1). Scanning the potential further into the positive potential range allows a further oxidation response to be observed (see P2) which is associated with the presence of glucose (as reducing agent) in the aqueous solution. The characteristic shape of this glucose oxidation process is caused by the electrocatalytic nature of gold towards glucose oxidation and this feature is consistent with literature reports.[22] Upon reversal of the scan direction, a further prominent peak response is observed at −0.8 V *vs.* SCE (see P3). This response is associated with the reductive dissolution of indigo from the electrode surface back into the solution phase. Closer inspection shows that there are two peak features associated with process P3 and this is in good agreement with data in Fig. 4A. The first reduction peak is linked to the fast surface reduction of indigo (fast surface process) and the second broader peak is associated with the follow-up dissolution kinetics (slow bulk process). The

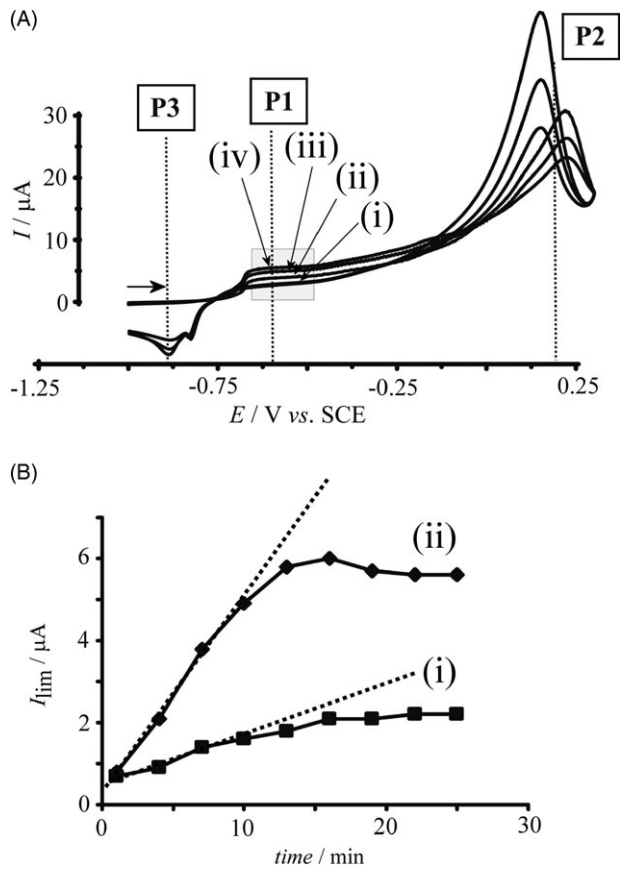

Fig. 5 (A) Cyclic voltammograms (scan rate 0.2 V s^{-1}) monitoring the glucose-driven reduction of 30 mg indigo (corresponding to 1.1 mM in 100 cm^3 aqueous 0.2 M NaOH) in the presence of 22 mM glucose at 65 °C (data taken every 3 min: (i) back scan, (ii) 4 min, (iii) 7 min, (iv) 10 min). (B) Plot of the limiting currents of the *leuco*-indigo oxidation *versus* time at (i) 0.1 M and (ii) 0.2 M NaOH.

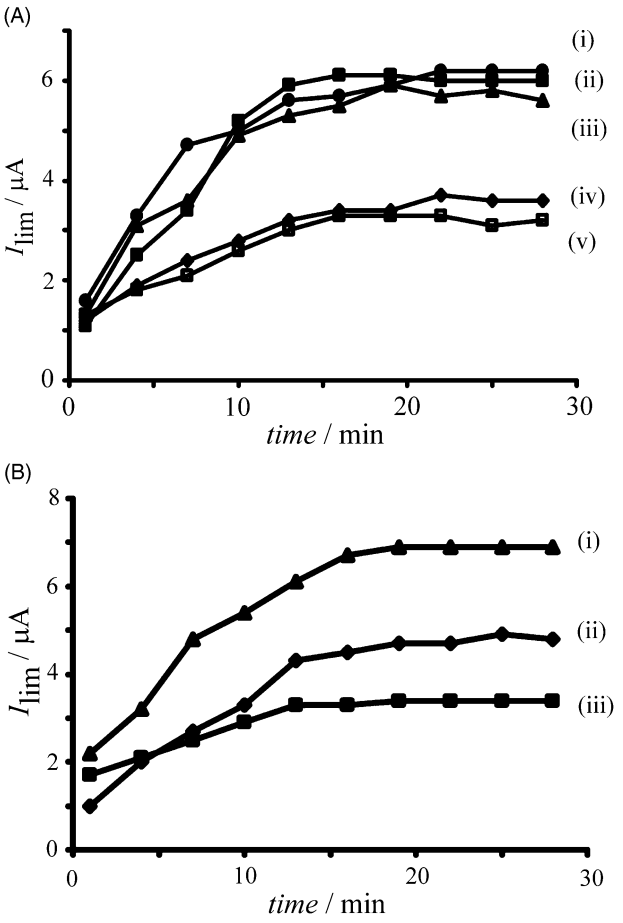

Fig. 6 (A) Plots of the limiting currents of the *leuco*-indigo oxidation *versus* time for the reduction of 30 mg of indigo (corresponding to 1.1 mM) with 22 mM glucose in 100 cm^3 aqueous 0.1 M NaOH at 65 °C. The concentration of anthraquinone (present as solid) was (i) 30 μM, (ii) 15 μM, (iii) 3.0 μM, (iv) 1.5 μM, and (v) 0.8 μM. (B) Plots of the limiting currents of the *leuco*-indigo oxidation *versus* time for the reduction of 30 mg of indigo (corresponding to 1.1 mM) with 22 mM glucose in 100 cm^3 aqueous NaOH at 65 °C in the presence of 15 μM anthraquinone with (i) 0.1 M, (ii) 0.08 M, and (iii) 0.05 M NaOH.

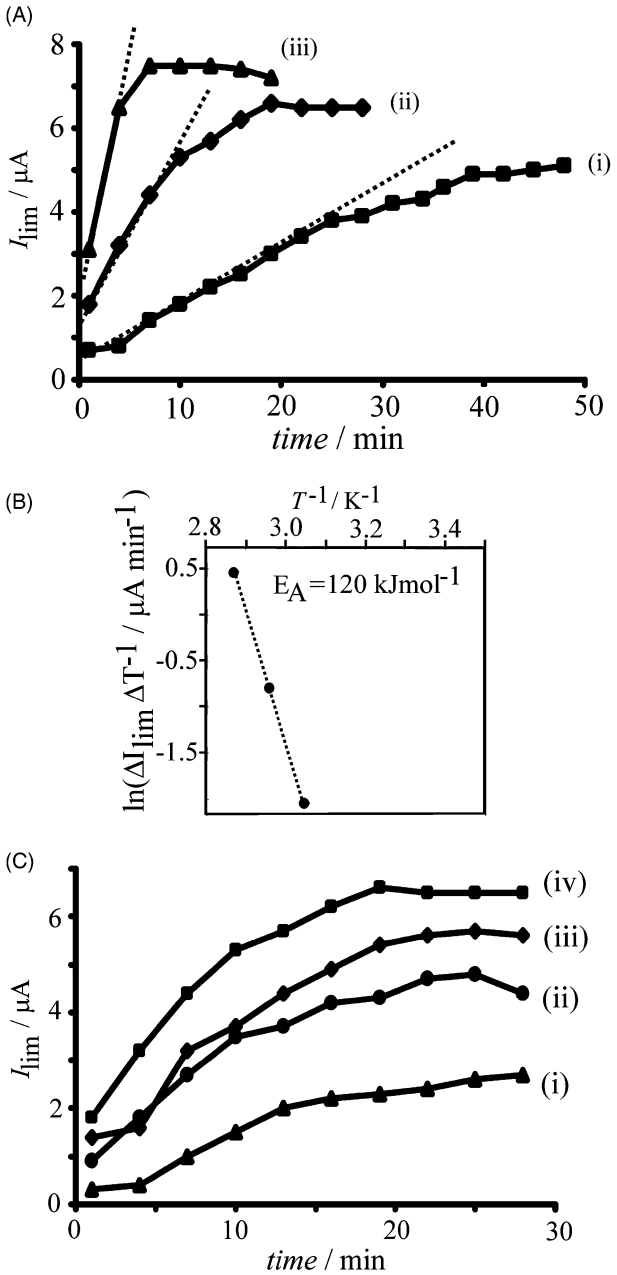

Fig. 7 (A) Plots of the limiting currents of the *leuco*-indigo oxidation *versus* time for the reduction of 30 mg of indigo (corresponding to 1.1 mM) with 22 mM glucose in 100 cm^3 aqueous 0.1 M NaOH at (i) 55 °C, (ii) 65 °C, and (iii) 75 °C. (B) Plots of the estimated reaction rate for *leuco*-indigo formation (see dotted lines in A) *versus* T^{-1}. (C) Plot of the limiting currents of the *leuco*-indigo oxidation *versus* time for the reduction of 30 mg of indigo (corresponding to 1.1 mM) with (i) 2.8 mM, (ii) 5.5 mM, (iii) 11 mM and (iv) 22 mM glucose in 100 cm^3 aqueous 0.1 M NaOH in the presence of 15μM anthraquinone and at 65 °C.

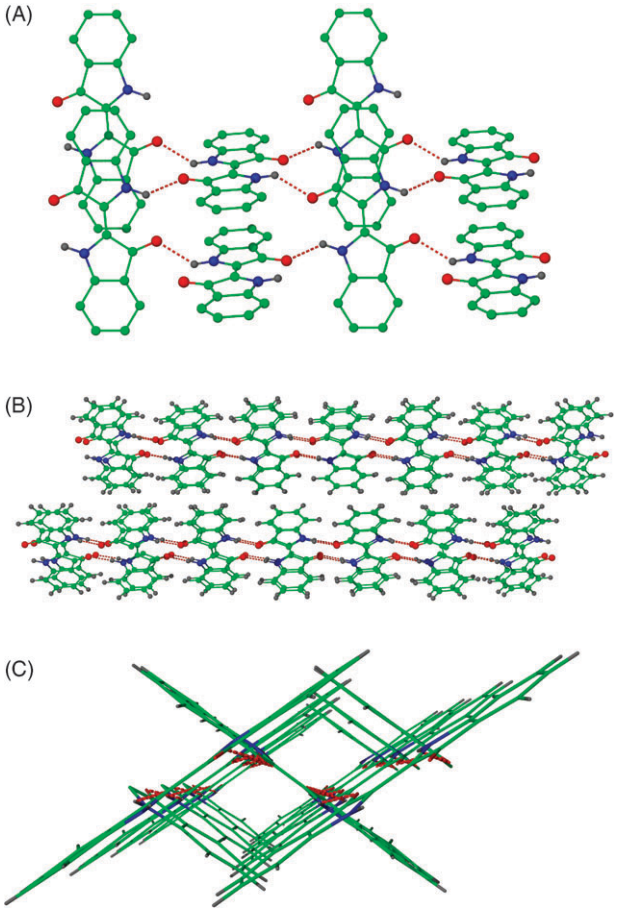

Fig. 8 Crystal structure[37] of indigo showing (A) from the top onto an indigo sheet, (B) from the side on two indigo sheets, and (C) from the side into a single indigo sheet. Within sheets, oxygen (red) and nitrogen (blue) atoms are inter-linked *via* hydrogen bonds (dashed lines).

experiment has to be conducted with a sufficiently fast scan rate in order to avoid blocking of the electrode due to formation of the indigo deposits.[24]

The limiting current plateau determined at −0.6 V *vs.* SCE is a direct measure of the *leuco*-indigo concentration. The formation of *leuco*-indigo in 0.2 M NaOH with time is shown in Fig. 5B. It can be seen that at 65 °C the *leuco*-indigo concentration increases steadily over a 10–15 min period after which it reaches a plateau. At this point the glucose-driven reduction is complete and the colour has changed from blue to orange. The slope of the initial time-course (see dotted line) represents the initial rate of *leuco*-indigo formation.[18] If the concentration of NaOH is lower (see Fig. 5Bii) the rate of *leuco*-indigo formation is severely reduced and the endpoint apparently different. The colour of the suspension in 0.1 M NaOH remains dark, consistent with incomplete conversion of indigo. Therefore, the concentration of NaOH is a crucial parameter in the effectiveness of the overall reduction process. It is possible that the ability of glucose to generate a powerful reducing agent depends on the level of hydroxide present in solution. Furthermore, the lack of progress in the reductive dissolution is also linked to the activity of Na^+ which is competing with protons for the anionic binding sites on the surface of the reacting indigo crystal (*vide infra*). In order to improve the rate and efficiency of the indigo reduction (while limiting the need for alkali during the process), redox catalysts can be introduced. One such redox catalyst as demonstrated in this study is anthraquinone.

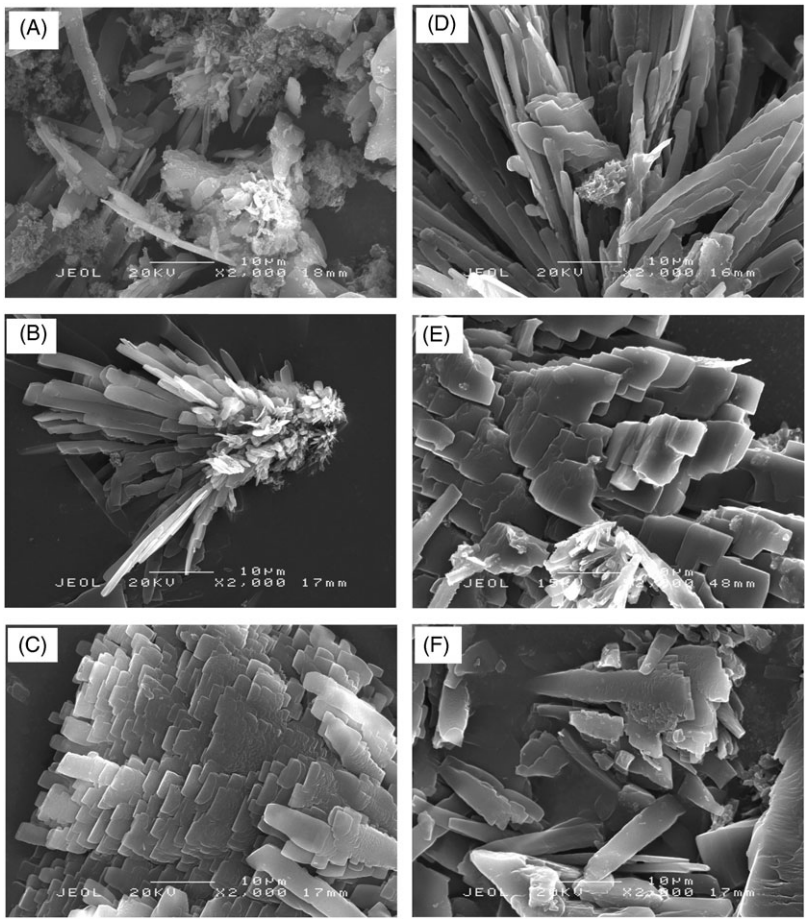

Fig. 9 SEM images (low magnification) of indigo crystals (A) before reduction, (B) after 3 min reduction, (C) after 14 min reduction, (D) anthraquinone-dosed after 3 min reduction, (E) anthraquinone-dosed after 15 min reduction, and (F) anthraquinone-dosed after 25 min reduction. The reduction was achieved by immersion into aqueous 0.2 M NaOH with 22 mM glucose at 65 °C which was followed by rinsing with water and drying.

3.3 Anthraquinone catalysis of the glucose-driven reduction of indigo to *leuco*-indigo

Anthraquinone derivatives are well-known redox mediator systems and they have been employed previously for the mediated reduction of indigo suspensions.[33] Perhaps surprisingly, anthraquinone derivatives also play an important catalytic role in the bacterial indigo reduction process.[4,5] Many anthraquinone derivatives are toxic but the parent anthraquinone is relatively safe to use[34] and readily available. The insignificant solubility of anthraquinone in aqueous media can be sidestepped in the present work by direct impregnation of the redox catalyst onto the indigo substrate prior to the reduction experiments. The anthraquinone catalyst was dissolved in acetone, indigo particles suspended into this solution by sonication, and after complete evaporation of the solvent, we obtained indigo on which anthraquinone had been uniformly immobilised. The amount of anthraquinone on the indigo surface was altered to determine the lowest effective level of catalyst.

Fig. 6A shows plots for the formation of *leuco*-indigo from anthraquinone-dosed indigo. In contrast to what happens in the absence of anthraquinone, the reduction process is highly effective in the presence of the lower concentration (0.1 M) of NaOH, and indigo is completely converted to *leuco*-indigo within 10–15 min (compare Fig. 5B). Low levels of anthraquinone effectively increase the rate and conversion level of the reduction process. At a level of 0.3 mol% (corresponding to 3 μM) the catalyst is still fully active and only at 0.1 mol% is the effect lost. In comparison, a solution of 3 μM water-soluble 1,8-dihydroxyanthraquinone catalyst was reported to have virtually no effect.[10] With insufficient amounts of anthraquinone (less than 3 μM) the indigo reduction process fails to go to completion and the suspension remains dark. Increased amounts of catalyst above the critical level do not significantly speed up the reduction process either (see Fig. 6A). Excess of anthraquinone catalyst is likely to remain insoluble and inactive under the reaction conditions employed.

These findings suggested that it would be profitable to determine if the NaOH concentration could be lowered even further in the presence of anthraquinone catalyst, but Fig. 6B demonstrates that lowering the concentration of NaOH significantly below 0.1 M is not compatible with the full reduction of indigo (at 65 °C). It was noted that the suspension remained dark and therefore the reduction incomplete even after the plateau level of *leuco*-indigo had been reached.

The rate of *leuco*-indigo formation was followed by voltammetry at temperatures of 55 °C, 65 °C, and 75 °C. The plots in

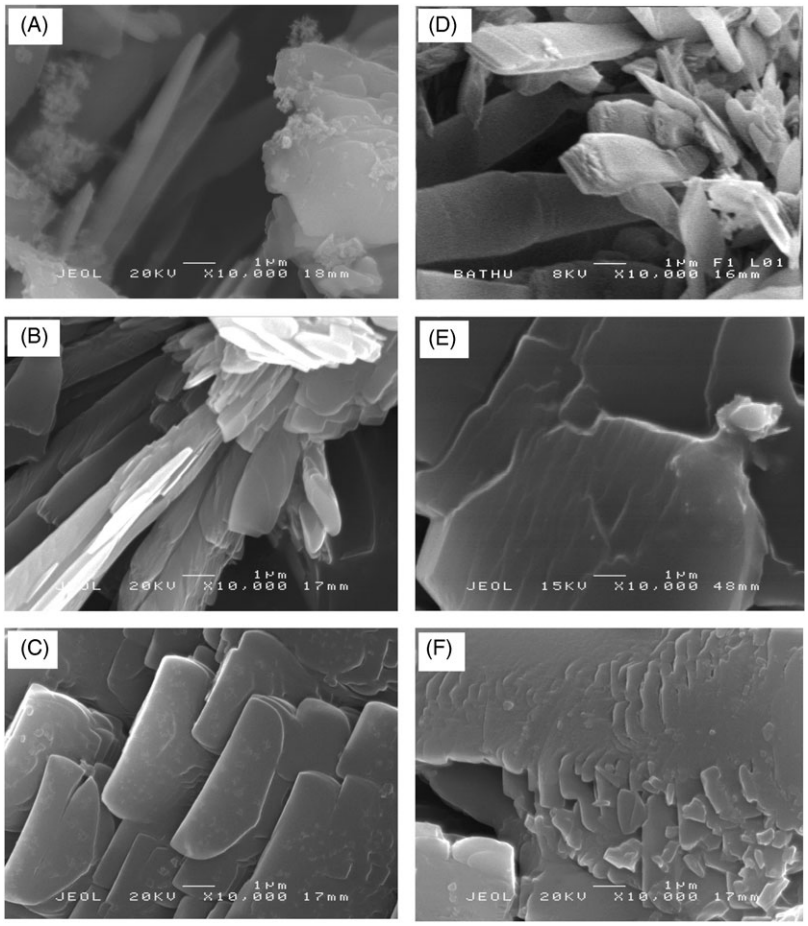

Fig. 10 SEM images (high magnification) of indigo crystals (A) before reduction, (B) after 3 min reduction, (C) after 14 min reduction, (D) anthraquinone-dosed before reduction, (E) anthraquinone-dosed after 15 min reduction, and (F) anthraquinone-dosed after 25 min reduction. The reduction was achieved by immersion into aqueous 0.2 M NaOH with 22 mM glucose at 65 °C which was followed by rinsing with water and drying.

Fig. 7A demonstrate the dramatic effect of temperature on the indigo reduction process. Increasing the temperatures significantly accelerates the reduction of indigo and from the approximate rate of *leuco*-indigo formation the Arrhenius activation energy can be estimated (see Fig. 7B).

The magnitude of the activation energy, 120 kJ mol^{-1}, is relatively high, and even after correction due a component introduced by the diffusion process of *leuco*-indigo, the activation energy is still indicative of a high activation barrier, almost twice as high as that observed for the same process in the absence of the anthraquinone catalyst.[24] A substantial part of the observed composite activation energy could be associated with the increase in solubility of the anthraquinone catalyst system.

Fig. 7C demonstrates the effect of the glucose concentration on the indigo reduction process. Glucose is present typically in 20-fold excess and halving the concentration of glucose appears to not affect significantly the progress of the reaction. Halving the concentration of glucose again, however, does affect the process. An excess of at least 10-fold of glucose *versus* indigo appears to be necessary for the reaction to go to completion (in the presence of 15 μM anthraquinone and at 65 °C).

3.4 Electron microscopy study of the glucose-driven reduction of indigo to *leuco*-indigo

In order to complement the kinetic data obtained in indigo suspension experiments, it was desirable to observe directly indigo crystals during the reduction. Indigo crystals of almost macroscopic size can be grown in short-path sublimation experiments (see experimental) to obtain plate-like crystals that owe their appearance to the layered packing in the indigo crystal structure. Indigo crystallises monoclinic and in space group $P2_1/c$.[35] Fig. 8 shows the indigo structure from three directions (red = O, blue = N, green = C) and the sheet-like structures held by the strong inter-molecular hydrogen bonds are clearly visible. The sheet structure at molecular level is reflected in the formation of thin crystal plates at macroscopic level. During the indigo reduction process, both the interactions between sheets and the stronger interactions within sheets need to be overcome.

Indigo crystals grown by sublimation were immobilised onto sticky carbon tape (for mounting SEM samples) and imaged by electron microscopy (after gold sputter coating). Fig. 9A shows a typical assembly of plate-like crystals with smaller crystal debris visible initially. The characteristic shape

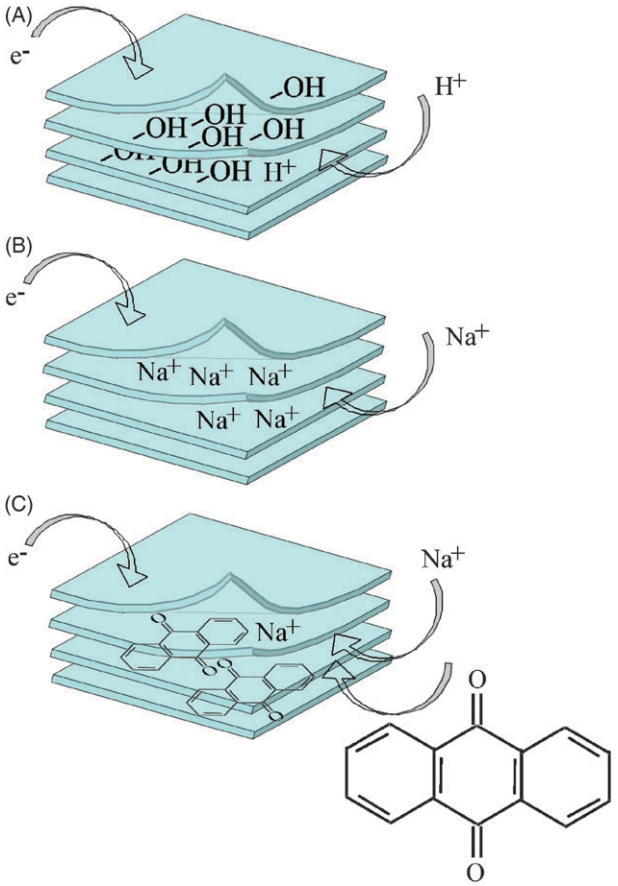

Fig. 11 Schematic representation of the indigo reduction process at the edge of a layered indigo crystal with (A) proton intercalation, (B) Na^+ intercalation, and (C) simultaneous anthraquinone and Na^+ intercalation.

of the crystals originates from the preferred growth direction planar to the sheet.

In order to monitor the indigo reduction, samples of immobilised indigo crystals were immersed in glucose-containing reduction solution and withdrawn at various times. Fig. 9B and C show samples after 3 min and after 14 min reduction. The smaller indigo crystal debris was immediately removed. Larger crystals remained and were still observed after 14 min of reduction.

When the experiment was repeated with anthraquinone-dosed indigo (see Fig. 9D–F) similar images to those obtained with untreated indigo were obtained. In all cases the plate-shape of indigo crystals remains and no holes are formed. It is therefore most likely that the reductive dissolution process occurs from the edges and that this process is relatively slow perpendicular to the indigo sheets. Closer inspection of Fig. 9C and F shows etch patterns and terrace-like features which are typical for reductive dissolution occurring from the edges.

Fig. 10 shows a set of higher magnification images. In the presence of anthraquinone there appear to be more irregular features possibly associated with local anthraquinone concentration variations. Although quantitative information is not obtained from these images, qualitatively they support the idea of a reductive dissolution process occurring at the edges of indigo crystals.

Fig. 11 shows a schematic representation of three types of reductive dissolution. In the presence of protons the reduction is limited to the edges of indigo sheets and proton intercalation followed by delamination and further dissolution is unlikely to occur. Protons are likely to be bound in the form of hydroxyl groups and therefore less likely to intercalate. A similar conclusion for related dye systems has been reached by Doménech *et al.* who employed *in situ* AFM[36] and chronoamperometry techniques.[37] Protons are believed "block" further progress of the reductive dissolution into the solid. In contrast, sodium cations can intercalate, which, under sufficiently alkaline conditions, will lead to slow delamination and disintegration of the indigo sheets. Finally, in the presence of anthraquinone, strong adsorption of the planar anthraquinone molecule into the gap between indigo sheets occurs and the catalyst is moving into the crystal like a "wedge" causing more rapid delamination and faster reductive dissolution.

Further and more quantitative kinetic studies are required to resolve the complex catalytic and dye dissolution processes in more detail. In future, advanced imaging techniques such *in situ* AFM monitoring[38] are most likely to provide further essential kinetic information.

4. Conclusions

It has been demonstrated that anthraquinone, although insoluble in water, is a highly effective catalyst in the glucose-driven reduction of indigo to *leuco*-indigo in aqueous 0.1 M NaOH. Anthraquinone is adsorbed/immobilised onto the indigo powder prior to the reduction. For indigo crystals of micron dimension, a molar ratio of 1 : 400 for anthraquinone : indigo is effective for complete conversion with 10-fold excess of glucose at 65 °C (corresponding to 3 μM anthraquinone). The temperature has a considerable effect on the anthraquinone-catalysed reductive dissolution ($E_A \approx 120$ kJ mol^{-1}). A molecular mechanism based on adsorption of anthraquinone between indigo sheets has been proposed to explain the remarkably enhanced reductive dissolution. Anthraquinone and Na^+ ions are believed to penetrate between the indigo sheets and thereby help break up the solid crystal. This conclusion reached from studies in which glucose was the origin of the reducing potential is consistent with studies of bacterial reduction[4,5] where it was concluded that the stimulatory effect of soluble anthraquinone derivatives on bacterial indigo reduction was best explained by an alteration of the surface properties of the bacteria or indigo particles.

Acknowledgements

A. V. thanks the Academy of Finland and Finnish Cultural Foundation for financial support.

References

1 K. G. Gilbert and D. T. Cooke, *Plant Growth Regul.*, 2001, **34**, 57.
2 A. Roessler and X. Jin, *Dyes & Pigments*, 2003, **59**, 223.
3 A. N. Padden, V. M. Dillon, P. John, J. Edmonds, M. D. Collins and N. Alvarez, *Nature*, 1998, **396**, 225.
4 S. K. Nicholson and P. John, *Biocatal Biotransform.*, 2004, **22**, 397.

5 S. K. Nicholson and P. John, *Appl. Microbiol. Biotechnol.*, 2005, **68**, 117.
6 M. A. Kulandainathan, K. Patil, A. Muthukumaran and R. B. Chavan, *Color. Technol.*, 2007, **123**, 143.
7 T. Bechtold, E. Burtscher, G. Kühnel and O. Bobleter, *J. Soc. Dyers Colour.*, 1997, **113**, 135.
8 A. Roessler and D. Crettenand, *Dyes & Pigments*, 2004, **63**, 29.
9 M. A. Kulandainathan, A. Muthukumaran, K. Patil and R. B. Chavan, *Dyes & Pigments*, 2007, **73**, 47.
10 A. Vuorema, P. John, A. T. A. Jenkins and F. Marken, *J. Solid State Electrochem.*, 2006, **10**, 865.
11 T. Bechtold and A. Turcanu, *J. Electrochem. Soc.*, 2002, **149**, D7.
12 T. Bechtold, E. Burtscher, A. Amann and O. Bobleter, *J. Chem. Soc., Faraday Trans.*, 1993, **89**, 2451.
13 T. Bechtold and A. Turcanu, *J. Appl. Electrochem.*, 2004, **34**, 1221.
14 T. Bechtold, E. Burtscher and A. Turcanu, *J. Electroanal. Chem.*, 1999, **465**, 80.
15 A. Roessler, D. Crettenand, O. Dossenbach and P. Rys, *J. Appl. Electrochem.*, 2003, **33**, 901.
16 A. Roessler, O. Dossenbach, W. Marte and P. Rys, *J. Appl. Electrochem.*, 2002, **32**, 647.
17 R. S. Blackburn and A. Harvey, *Environ. Sci. Technol.*, 2004, **38**, 4034.
18 A. Vuorema, P. John, M. Keskitalo, M. A. Kulandainathan and F. Marken, *Dyes & Pigments*, 2008, **76**, 542.
19 R. J. Ferrier and P. M. Collins, *Monosaccharide chemistry*, Penguin Books, Harmondsworth, 1972, ch. 3, p. 89.
20 J. M. De Bruijn, A. P. G. Kieboom and H. van Bekkum, *Starch/Stärke*, 1987, **39**, 23.
21 J. M. De Bruijn, A. P. G. Kieboom and H. van Bekkum, *Sugar Technol. Rev.*, 1986, **13**, 21.
22 M. A. Ghanem, R. G. Compton, B. A. Coles, A. Canals, A. Vuorema, P. John and F. Marken, *Phys. Chem. Chem. Phys.*, 2005, **7**, 3552.
23 G. Matricali, M. M. Dieng, J. F. Dufeu and M. Guillou, *Electrochim. Acta*, 1976, **21**, 943.
24 A. Vuorema, P. John, M. Keskitalo and F. Marken, *J. Appl. Electrochem.*, 2008, **38**, 1683.
25 T. Grygar, F. Marken, U. Schröder and F. Scholz, *Collect. Czech. Chem. Commun.*, 2002, **67**, 163.
26 A. M. Bond, F. Marken, C. T. Williams, D. A. Beattie, T. E. Keyes, R. J. Forster and J. G. Vos, *J. Phys. Chem. B*, 2000, **104**, 1977.
27 S. J. Holt and P. W. Sadler, *Proc. Royal Soc. London, Ser. B*, 1958, **148**, 495.
28 J. N. Etters, *J. Soc. Dyers Colour.*, 1993, **109**, 251.
29 T. Vickerstaff, *The physical chemistry of dyeing*, Oliver and Boyd, London, 1954, ch. IX.
30 A. M. Bond, F. Marken, E. Hill, R. G. Compton and H. Hügel, *J. Chem. Soc. Perkin Trans. II*, 1997, **9**, 1735.
31 A. Domenech, M. T. Domenech-Carbo and M. L. V. de Agredos Pascual, *J. Phys. Chem. C*, 2007, **111**, 4585.
32 T. Grygar, S. Kuckova, D. Hradil and J. Hradilova, *J. Solid State Electrochem.*, 2003, **7**, 706.
33 T. Bechtold, E. Burtscher and A. Turcanu, *J. Electroanal. Chem.*, 1999, **465**, 80.
34 *The Merck Index*, ed. S. Budavari, Merck & Co., New Jersey, 12th edn, 1996.
35 P. Suesse, M. Steins and V. Kupcik, *Z. Kristallographie*, 1988, **184**, 269.
36 A. Doménech and M. T. Doménech-Carbo, *Electrochem. Commun.*, 2008, **10**, 1238.
37 A. Doménech and M. T. Doménech-Carbo, *J. Solid State Electrochem.*, 2006, **10**, 949.
38 S. R. Higgins, L. H. Boram, C. N. Eggleston, B. A. Coles, R. G. Compton and K. G. Knauss, *J. Phys. Chem. B*, 2002, **106**, 6696.

